Adiabatic Water Suppression Using Frequency Selective Excitation

Robin A. de Graaf, Klaas Nicolay

A new method for B_1-insensitive water suppression using adiabatic RF pulses is described. The transition zone of the inversion profile of adiabatic full passage (AFP) pulses is used for frequency-selective excitation followed by dephasing of the excited water with magnetic field gradients. Several improvements of AFP pulses, which also have implications for other applications, are described. The technique was evaluated by simulations based on the Bloch equations (including relaxation), *in vitro* experiments and an *in vivo* verification on neonatal and adult rat brain.

Key words: water suppression; B_1-insensitive; adiabatic full passage pulses.

INTRODUCTION

Proton magnetic resonance spectroscopy (^{1}H MRS) of metabolites in the millimolar concentration range is complicated by the overwhelming water resonance. In recent years a wide range of water suppression techniques has been developed (1–11, for reviews see 12–14). All techniques utilize a difference between water and metabolites which is reflected in a NMR parameter. These include differences in longitudinal and/or transverse relaxation, diffusion, scalar coupling, and chemical shift. The most popular water suppression techniques for *in vivo* ^{1}H MRS are almost all based on a difference between the resonance frequencies of water and metabolites and include frequency selective excitation of the water followed by magnetic field gradient dephasing (5, 6, 12–14), presaturation (1), selective spin-echo dephasing (9–11), non-excitation/refocusing of the water (3, 4) and nulling of the water by selective inversion (i.e., selective WEFT) (2). However, none of these water suppression methods functions optimally under all possible experimental conditions. Presaturation (1) may lead to unacceptable RF power deposition and distorts the metabolite resonance intensities by magnetization transfer effects (15, 16). Selective spin-echo dephasing methods (9–11) give excellent water suppression but result in considerable prolongation of the minimum echo-time TE (> 30 ms). Non-excitation of the water by binomial RF pulses is often accompanied by a non-ideal excitation profile for the metabolite resonances (3, 4) and selective WEFT can only give optimal suppression for one particular value of the longitudinal relaxation time constant (2). These considerations have made chemical shift selective excitation followed by magnetic field gradient dephasing (i.e., CHESS) the most popular water suppression technique for short echo-time ^{1}H MRS.

In vivo ^{1}H MRS is often executed with surface coils to increase the sensitivity and achieve crude spatial localization. When the surface coil is also used for the transmission of conventional (amplitude-modulated) RF pulses, the intrinsic B_1-inhomogeneities largely determine the success of water suppression, making it desirable to use a B_1-insensitive (adiabatic) pulse sequence. Several adiabatic solvent suppression techniques have been developed (17–20), which are often closely related to techniques executed with conventional amplitude-modulated RF pulses. For example, SSAP (solvent *s*uppression *a*diabatic *p*ulse) is a direct adiabatic analogue of a jump-return pulse (17, 19). However, the absence of a frequency-selective adiabatic excitation pulse has prevented the implementation of an adiabatic analogue of the CHESS water suppression sequence.

Here we propose an adiabatic water suppression technique based on the CHESS pulse sequence, by utilizing the characteristic frequency profile of adiabatic full passage RF pulses for frequency selective excitation. This technique, which we named SWAMP (*s*equence for *w*ater suppression with *a*diabatic *m*odulated *p*ulses) has an excellent insensitivity to B_1-inhomogeneities, induces no spectral distortions outside the water region, is easy to implement, and allows short echo-time ^{1}H MRS.

THEORY

Adiabatic RF pulses are characterized by simultaneous modulation of RF amplitude, $B_1(t)$, and frequency, $\Delta\omega(t) = \omega(t) - \omega_0$, where ω_0 is the Larmor frequency. The modulation functions can be described in terms of normalized functions $f_B(t)$ and $f_\omega(t)$, according to

$$B_1(t) = B_{1max} f_B(t) \quad [1]$$

$$\Delta\omega(t) = \Delta\omega_{max} f_\omega(t) \quad [2]$$

where B_{1max} and $\Delta\omega_{max}$ are the maximum RF amplitude and frequency modulation (relative to the Larmor frequency ω_0) values, respectively. The pulse may also be executed with phase (instead of frequency) modulation by calculating the time integral of the frequency modulation (21, 22). The $B_1(t)$ and $(\Delta\omega(t)/\gamma)$ magnetic field vectors together generate an effective magnetic field vector $B_e(t)$, whose amplitude and direction are given by

$$B_e(t) = \sqrt{B_1^2(t) + \left(\frac{\Delta\omega(t)}{\gamma}\right)^2} \quad [3]$$

MRM 40:690–696 (1998)

From the Department of Experimental *In Vivo* NMR, Image Sciences Institute and Bijvoet Center, Utrecht University, The Netherlands.

Address correspondence to: Robin A. de Graaf, Department of Experimental *in vivo* NMR, Image Sciences Institute and Bijvoet Center, Utrecht University, Bolognalaan 50, 3584 CJ, Utrecht, The Netherlands.

Received April 16, 1998; revised July 17, 1998; accepted July 17, 1998.

0740-3194/98 $3.00

and

$$\alpha(t) = \arctan\left(\frac{\Delta\omega(t)}{\gamma B_1(t)}\right) \qquad [4]$$

respectively. $\alpha(t)$ defines the angle between $B_e(t)$ and transverse plane of the frequency frame $x'y'z'$ (which rotates about z' at the instantaneous frequency $\omega(t)$ of the RF pulse). The rotation of magnetization M during an adiabatic RF pulse is inherently linked to the rotations of the effective field $B_e(t)$. For instance, magnetization vectors parallel to $B_e(t)$ will remain like that throughout the pulse (independent of the RF amplitude) and the trajectory of M can be deduced by following the rotations of the effective field $B_e(t)$. However, if the rate of change of $B_e(t)$, i.e., $(d\alpha(t)/\gamma dt)$, is comparable or larger than the amplitude of $B_e(t)$, then the actual effective magnetic field is the vector sum of $B_e(t)$ and $(d\alpha(t)/\gamma dt)$ and M will rotate about $B_e(t)$ as a complex function of RF amplitude and frequency offset. Therefore, if the adiabatic condition, defined as

$$\left|\frac{d\alpha(t)}{dt}\right| \ll |\gamma B_e(t)| \qquad [5]$$

is satisfied, magnetization vectors retain their orientation (i.e., parallel or perpendicular) to the effective field, making the rotation independent of the RF amplitude.

Although many modulation functions $f_B(t)$ and $f_\omega(t)$ satisfy the adiabatic condition, an adiabatic full passage (AFP) pulse is often executed with $f_B(t)$ and $f_\omega(t)$ chosen according to a complex hyperbolic secant function

$$f_B(t) = \mathrm{sech}\left[\beta\left(\frac{2t}{T} - 1\right)\right] \quad 0 \le t \le T \qquad [6]$$

$$f_\omega(t) = \tanh\left[\beta\left(\frac{2t}{T} - 1\right)\right] \quad 0 \le t \le T \qquad [7]$$

where β is defined for a 1% cut-off level, i.e., $\mathrm{sech}(\beta) = 0.01$. Eqs. [6] and [7] define the well-known Silver-Hoult hyperbolic secant AFP pulse ((23), Figs. 1a and 1b), which achieves a frequency selective inversion, independent of the RF amplitude above a minimum threshold RF amplitude (Figs. 1c and 1d). The frequency selective inversion profile has made this pulse popular in spatial localization (24), water suppression (20), and (wideband) decoupling (25) applications.

All simulations presented in this article are based on the classical Bloch equations in the standard rotating frame (e.g., rotating at the Larmor frequency ω_0). Individual AFP pulses were segmented in 2048 intervals over which the RF amplitude and phase modulation was assumed constant. The Bloch equations (in which B_0 magnetic field gradients and T_1 and T_2 relaxation were optional) were numerically integrated using a fourth order Runge-Kutta algorithm. Complete (macroscopic) dephasing was assumed during B_0 magnetic field gradients. For 1D and 2D simulations 2000 and 200 × 400 points were calculated, respectively.

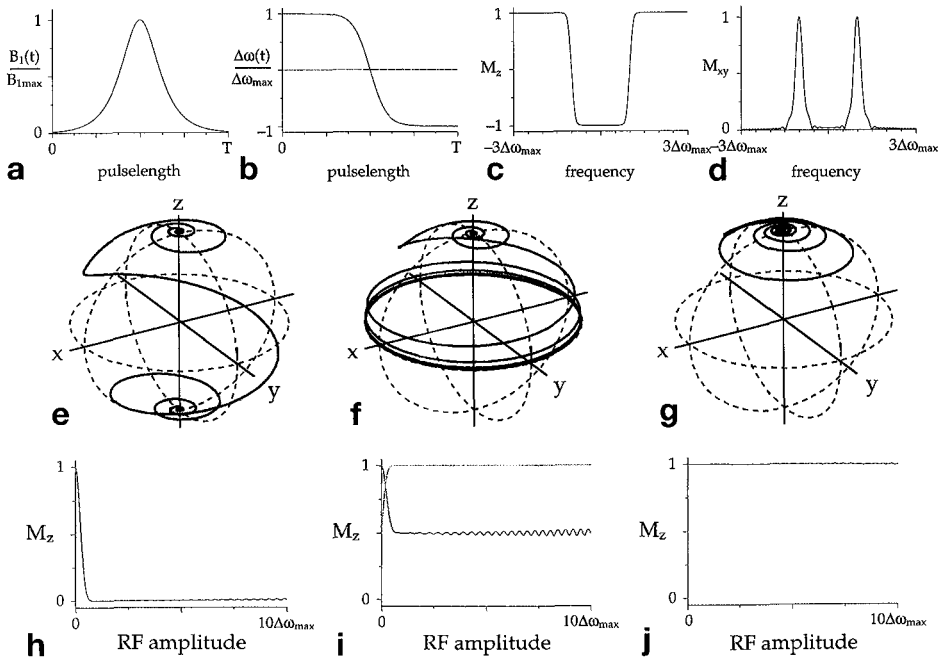

FIG. 1. (a) RF amplitude and (b) frequency modulation functions of a hyperbolic secant AFP pulse (Eqs. [1] and [2]). (c) Longitudinal and (d) transverse magnetization following the AFP pulse shown in (a) and (b) for $\gamma B_{1max} = \Delta\omega_{max}$. (e–g) Rotations of the (initially) longitudinal magnetization in the standard rotating frame during an AFP pulse for frequency offsets $\Delta\Omega$ of (e) $0.5\Delta\omega_{max}$, (f) $\Delta\omega_{max}$ and (g) $1.5\Delta\omega_{max}$. (h–j) B_1 dependence of the longitudinal magnetization following an AFP pulse at frequency offsets (h) $0.5\Delta\omega_{max}$, (i) $\Delta\omega_{max}$ and (j) $1.5\Delta\omega_{max}$. The B_1 dependence of the transverse magnetization is also shown for $\Delta\Omega = \Delta\omega_{max}$ (dotted) line in (i). The origin and removal of the small oscillations in (h–j) are described in the text.

Figures 1e–1g show the rotations of the longitudinal magnetization in the rotating frame for $\gamma B_{1max} = \Delta\omega_{max}$ and frequency offsets of $0.5\Delta\omega_{max}$ (inside the inversion band), $\Delta\omega_{max}$ (in the inversion transition), and $1.5\Delta\omega_{max}$ (outside the inversion band), respectively. Figures 1h–1j show the B_1 dependence of the rotation of the longitudinal magnetization for the frequency offsets $0.5\Delta\omega_{max}$, $\Delta\omega_{max}$, and $1.5\Delta\omega_{max}$, respectively. As described previously (21, 22 and references therein), the longitudinal magnetization follows the rotation of the effective field (i.e., the adiabatic condition is satisfied), leading to an inversion for $|\Delta\Omega| < |\Delta\omega_{max}|$ and a return to the initial orientation for $|\Delta\Omega| > |\Delta\omega_{max}|$. However, as can be seen from Figs. 1f and 1i, the adiabatic condition is also satisfied for

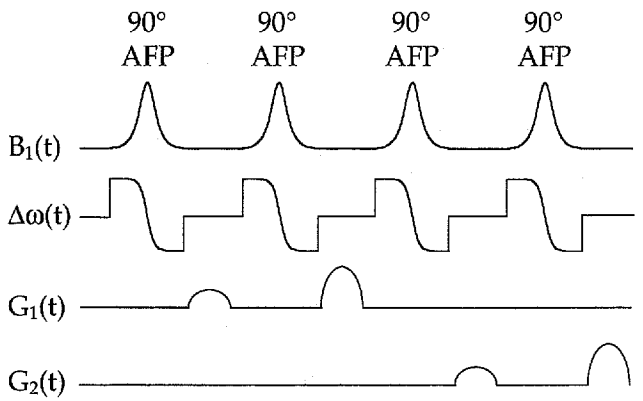

FIG. 2. SWAMP water suppression pulse sequence. An even number of AFP pulses for excitation of the water resonance is interleaved with (orthogonal) magnetic field gradients to dephase the excited water.

$\Delta\Omega = \Delta\omega_{max}$, leading to excitation of longitudinal magnetization. Essentially, the AFP pulse can be seen as an adiabatic half passage (AHP) excitation pulse at $\Delta\Omega = \Delta\omega_{max}$. Note, that at $\Delta\Omega = -\Delta\omega_{max}$, the pulse is equivalent to a time-reversed adiabatic half passage (RAHP) pulse. Although a RAHP pulse induces a RF amplitude and frequency offset dependent phase shift during excitation, it nevertheless satisfies the adiabatic condition of Eq. [5], such that the rotation of the longitudinal magnetization vector onto the transverse plane is completely B_1 insensitive. In conclusion, an AFP pulse achieves B_1 insensitive inversion for $|\Delta\Omega| < |\Delta\omega_{max}|$, excitation for $|\Delta\Omega| = \sim|\Delta\omega_{max}|$ and no net rotation for $|\Delta\Omega| > |\Delta\omega_{max}|$.

The B_1 insensitive, frequency-selective excitation of an AFP pulse can be used for adiabatic water suppression according to the pulse sequence shown in Fig. 2, which is referred to as SWAMP (*s*equence for *w*ater suppression with *a*diabatic *m*odulated *p*ulses). With SWAMP water suppression, an even number (four in the case of Fig. 2) of AFP pulses is interleaved with magnetic field gradients for dephasing of excited water. An even number of AFP pulses is recommended, such that a double inversion for $|\Delta\Omega| < |\Delta\omega_{max}|$ leads to a net rotation of 360° and signal is only removed for $|\Delta\Omega| = \sim|\Delta\omega_{max}|$.

Figure 3a shows a simulation based on the Bloch equations for the SWAMP sequence shown in Fig. 2 with AFP pulse length $T = 15$ ms and $\Delta\omega_{max}| = 667$ Hz. It follows that the removal of longitudinal magnetization is completely B_1 insensitive for $|\Delta\Omega| = \sim|\Delta\omega_{max}|$ for $\gamma B_{1max} > \sim 250$ Hz. However, the longitudinal magnetization is also partially excited for $|\Delta\Omega| \neq |\Delta\omega_{max}|$, especially at higher RF amplitudes. Following extensive simulations and experimental verification it turned out that this was caused by the 1% cut-off level of the RF amplitude modulation (i.e., $\text{sech}(\beta) = 0.01$) in Eq. [6]. Through the abrupt change in B_1 modulation at the start and the end of the hyperbolic secant AFP pulse, the adiabatic condition is not satisfied. This will lead to a rotation of M about the effective field and hence partial excitation of M even when $|\Delta\Omega| \neq |\Delta\omega_{max}|$. These undesirable rotations are also the cause of the small oscillations in Figs. 1h–1j. This suggests changing the RF amplitude modulation of Eq. [6]

$$B_1(t) = B_{1max}(f_B(t) - f_B(0)) \qquad [8]$$

Figure 3b shows the same simulation as in Fig. 3a, but now for AFP pulses executed with Eqs. [7] and [8]. The subtraction of the constant 1% cut-off level results in a clean selection of two frequency bands in which the longitudinal magnetization has been obliterated. The transformation from Eq. [6] to [8] is highly recommended for all applications involving hyperbolic secant pulses (or in general of adiabatic pulses with modulation functions exhibiting a cut-off level). For instance, the improved frequency profile of the adapted AFP pulse requires lower magnetic field crusher gradients during spatial localization, the out-of-slice signal contamination is lower and the in-slice signal loss has been reduced.

One of the most important characteristics of SWAMP water suppression is the suppression bandwidth, which is proportional to the transition width of the frequency selective inversion profile generated by the AFP pulse. Figure 3b shows that the transition width generated by the modified hyperbolic secant AFP pulse increases with increasing RF amplitude. This may be undesirable for certain applications. As stated earlier, many modulation functions $f_B(t)$ and $f_\omega(t)$ satisfy the adiabatic condition of Eq. [5]. It should therefore be possible to construct modulation functions which exhibit a sharper transition bandwidth. A particularly rigorous method to construct modulation functions for AFP pulses is the method of offset independent adiabaticity (OIA) (26). With the OIA method the adiabatic condition is analytically evaluated to allow the construction of AFP modulation functions which satisfy the adiabatic condition independent of the frequency offset. It was found that a Lorentzian modulated AFP pulse gave the sharpest transition zone. The $f_B(t)$ and $f_\omega(t)$ functions for a Lorentzian modulated AFP pulse are given by

$$f_B(t) = \frac{1}{1 + \beta\left(\frac{2t}{T} - 1\right)^2} \quad 0 \le t \le T \qquad [9]$$

$$f_\omega(t) = \frac{\left(\frac{2t}{T} - 1\right)}{\left(1 + \beta\left(\frac{2t}{T} - 1\right)^2\right)} + \frac{1}{\sqrt{\beta}}\arctan\left(\sqrt{\beta}\left(\frac{2t}{T} - 1\right)\right) \quad 0 \le t \le T \qquad [10]$$

where $\beta = 99$ (i.e., set on a 1% cut-off level). To achieve an optimal frequency profile, the RF amplitude modula-

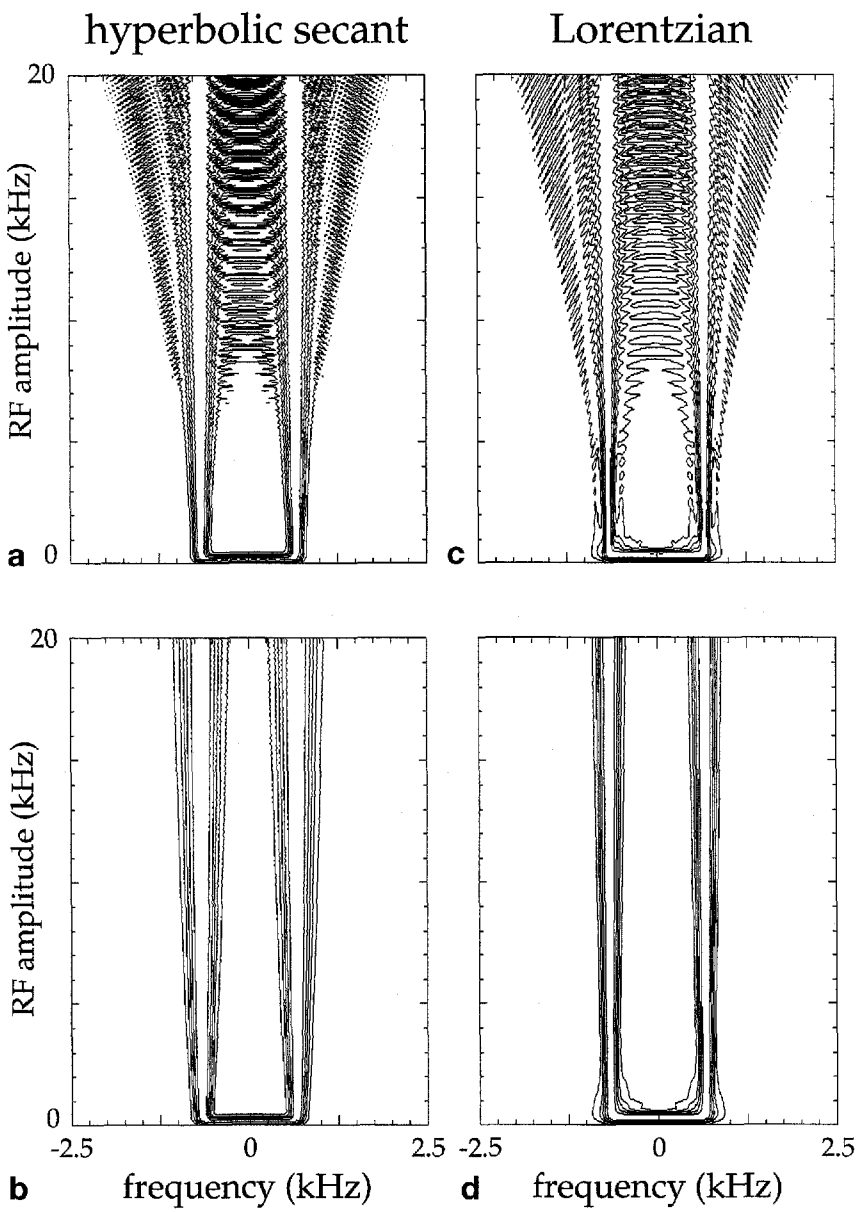

FIG. 3. Simulations of the longitudinal magnetization based on the Bloch equations of SWAMP water suppression executed with (a/b) hyperbolic secant and (c/d) Lorentzian modulated AFP pulses. The contour levels are drawn at 10, 30, 50, 70, and 90% of the longitudinal magnetization. (a/c) AFP pulses with a 1% RF amplitude cut-off level give rise to undesirable excitation during SWAMP, which is absent (b/d) when the cut-off level has been removed according to Eq. [8].

tion of Eq. [9] should be modified according to Eq. [8]. Figures 3c and 3d show simulations for a Lorentzian modulated AFP pulse. The suppression bandwidth is narrower and remains virtually constant over a large RF amplitude range. Due to the higher peak power of the Lorentzian AFP pulse, the minimum RF amplitude for optimal suppression is slightly higher than for a hyperbolic secant AFP pulse. In general, the suppression bandwidth of SWAMP water suppression can be changed by changing (1) the pulse length, (2) the (bandwidth × pulse length) product, (3) the modulation functions of the AFP pulses and (4) the number of AFP pulses. In all cases, the exact bandwidth can only be determined experimentally or by simulations based on the Bloch equations.

METHODS

All experiments were performed on a Varian/SIS Co console interfaced to a 4.7 T Oxford magnet equipped with a high-performance gradient insert (220 mT/m in 300 μs). *In vitro* experiments were performed on a water-filled sphere (Ø 16 mm) with a 4 turn solenoidal coil (Ø 20 mm, 40 mm length) tuned to the proton frequency (200 MHz). *In vivo* experiments were performed on neonatal (2–3 days) or adult male Wistar rats, anaesthetized with N_2O/O_2 (7:3) and 0.8% halothane. Spatial localization on neonatal rats was achieved with point resolved spectroscopy (PRESS, TR = 5000 ms, TE = 20 ms, 64 μl, NEX = 128), while on adult rats an adiabatic integrated OVS-ISIS (19) sequence (TR = 5000 ms, TE = 20 ms, 125 μl, NEX = 128) was employed. In the first case RF transmission was achieved with a Helmholtz coil and RF reception with a inductively coupled surface coil (Ø 20 mm), while for the adiabatic sequence the surface coil was used for both RF transmission and reception. SWAMP water suppression was achieved as shown in Fig. 2 with T = 15 ms and 1 ms 50 mT/m magnetic field crusher gradients (in a 1:2 ratio in two orthogonal directions). The suppression band at $\Delta\Omega = +\Delta\omega_{max}$ was used for water suppression. The frequency of the suppression band was set on the water resonance by changing the RF transmitter frequency. Alternatively, the pulse may be executed with an appropriate linear phase ramp.

RESULTS

Figure 4 shows the experimental verification of SWAMP water suppression. The result of conventional CHESS water suppression is shown as a reference. Figures 4a and 4b show the RF amplitude dependence of CHESS and SWAMP, respectively. The CHESS water suppression sequence gives only acceptable results over a very narrow RF amplitude range, whereas SWAMP achieves signal suppression independent of the RF amplitude, above a minimum threshold of ~250 Hz. Note that the

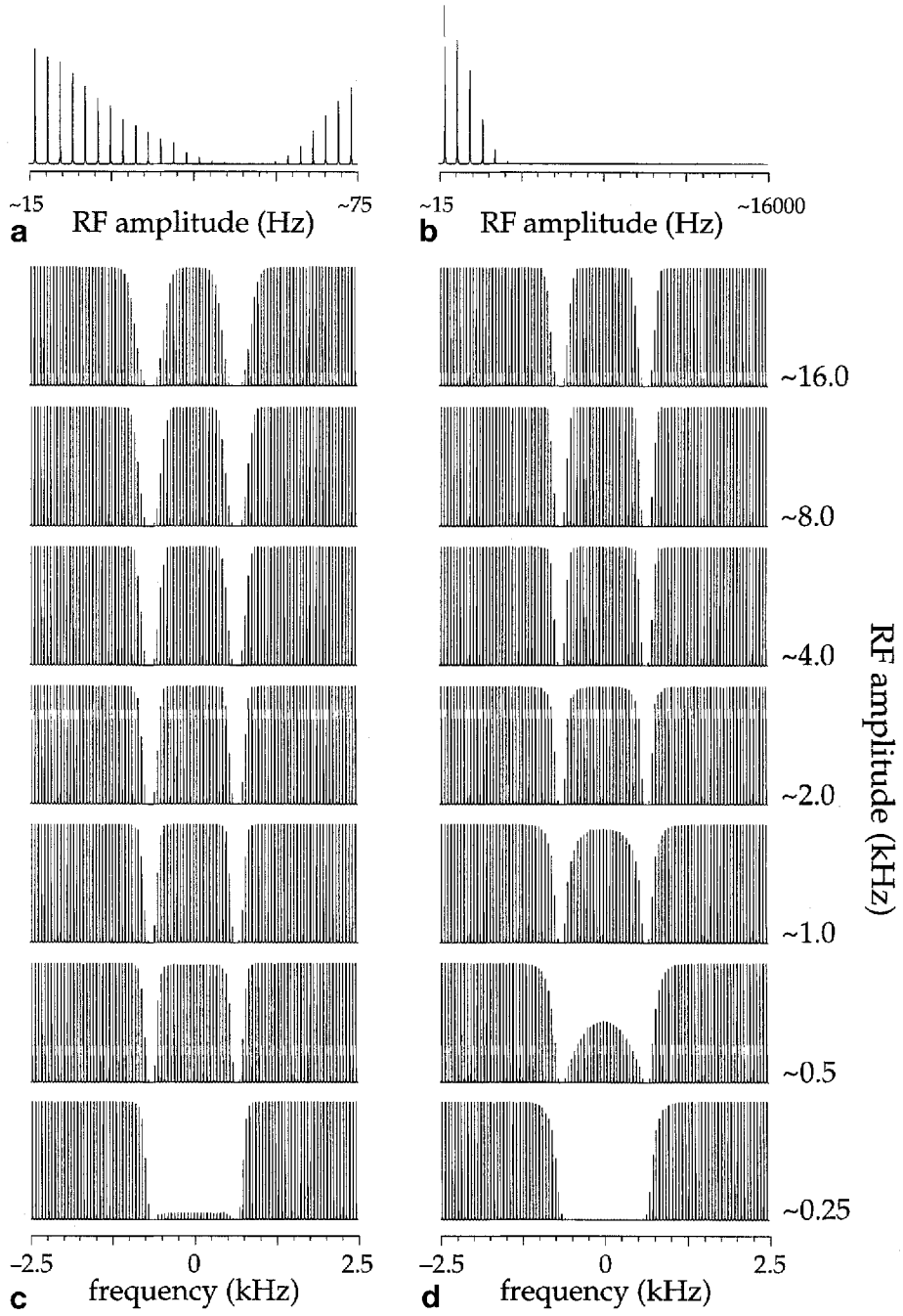

FIG. 4. Experimental verification of CHESS and SWAMP water suppression using a homogeneous 4-turn solenoidal RF coil for transmission and reception and a water-filled sphere. (a) CHESS water suppression (three 15-ms Gaussian RF pulses) and (b) SWAMP water suppression with 15 ms hyperbolic secant AFP pulses ($\Delta\omega_{max}$ = 667 Hz). (c) and (d) show SWAMP water suppression as a function of the RF amplitude and frequency offset for hyperbolic secant and Lorentzian AFP pulses, respectively; 101 spectra between −2.5 kHz and +2.5 kHz from the water resonance were acquired.

horizontal axis in both figures is logarithmic and that the RF amplitude range for SWAMP is >250 times that for conventional CHESS. Figures 4c and 4d show the off resonance performance of hyperbolic secant and Lorentzian modulated SWAMP, respectively. Due to the higher peak power of the Lorentzian AFP pulse, the minimum RF amplitude for optimal suppression is slightly higher than for a hyperbolic secant AFP pulse. Figure 5 shows an *in vivo* example of hyperbolic secant-modulated SWAMP water suppression. The spectra in Figs. 5a and 5b were obtained from neonatal rat brain at γB_{1max} = ~700 Hz and γB_{1max} = ~2800 Hz, respectively. Figures 5c and 5d show ^{1}H NMR spectra from adult rat brain with a Lorentzian-modulated SWAMP sequence (γB_{1max} ~ 4000 Hz). The double inversion caused by two AFP pulses during SWAMP ensures that magnetization is essentially unaffected for $|\Delta\Omega| < |\Delta\omega_{max}|$. As a result, metabolites downfield from the water resonance can also be observed. The comparison of Figs. 5c and 5d demonstrates that intermediates of the purine nucleotides degradation pathway were increased following global ischemia, as previously reported (27).

DISCUSSION

The absence of an adiabatic, frequency-selective excitation pulse has led to a range of B_1 insensitive water suppression techniques which achieve signal excitation in an alternative manner, like binomial excitation with SSAP (17, 19, 21, 22) or BIRIANI (18). SWAMP utilizes the transition zone of AFP pulses to achieve frequency selective excitation. When used in combination with magnetic field gradients, SWAMP achieves water suppression in close analogy to CHESS, i.e., repeated excitation of the water resonance followed by dephasing of transverse magnetization. Since the magnetization of the metabolites remains along the longitudinal axis, SWAMP may become an important element of short echo-time ^{1}H MRS applications, especially with inhomogeneous B_1 fields as encountered with surface coils. However, SWAMP is not limited to surface coil applications. The B_1 insensitivity of SWAMP can also be used in combination with homogeneous RF coils to eliminate the time-consuming RF amplitude calibration of existing water suppression techniques, like CHESS (e.g., see Figs. 5a and 5b).

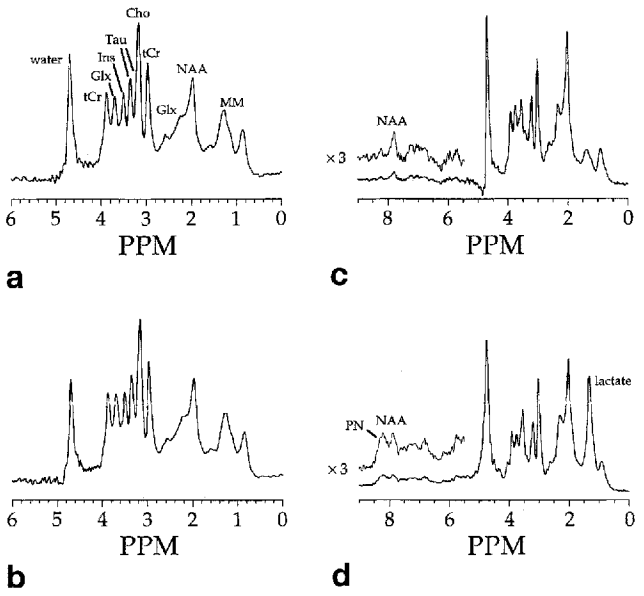

FIG. 5. *In vivo* ^{1}H MR spectra (TR = 5000 ms, TE = 20 ms, NEX = 128) obtained from (a/b) neonatal and (c/d) adult rat brain with SWAMP water suppression. An increase in the RF amplitude for SWAMP water suppression from (a) ~700 Hz to (b) ~2800 Hz did not significantly alter the spectrum, indicating the excellent insensitivity of SWAMP to B_1 inhomogeneities. ^{1}H MR spectra in (c) and (d) were acquired *in vivo* and postmortem, respectively, using surface coil transmission and reception and an adiabatic localization scheme (19) at $\gamma B_{1max} \sim 4000$ Hz. Abbreviations are for total creatine (tCr, i.e., creatine and phosphocreatine), glutamate/glutamine (Glx), *myo*-inositol (Ins), taurine (Tau), choline-containing compounds (Cho), *N*-acetylaspartate (NAA), macromolecules (MM) and purine nucleotides (PN).

The results presented here were for SWAMP using hyperbolic secant, and alternatively using Lorentzian AFP pulses. The former achieves suppression over a relatively large frequency band and at low RF amplitudes, while the Lorentzian based sequence suppresses a relatively narrow frequency band at higher RF amplitudes. It is, in principle, possible to optimize the modulation functions to combine both desirable features into one AFP pulse. Potential techniques to achieve this goal are given by the methods of OIA (26) and numerically optimized modulation (28), both of which use the adiabatic condition of Eq. [5] to optimize the modulation functions. However, for the purpose of this study, the described modulation functions (i.e., Eqs. [6]–[10]) achieved excellent water suppression over an adequate RF amplitude range.

The degree of water suppression which can be achieved with frequency-selective excitation sequences like SWAMP is largely determined by B_1 inhomogeneities and (longitudinal) relaxation. The adiabatic character of SWAMP ensures that the water suppression is not compromised by B_1 inhomogeneities (e.g., see Figs. 3–5). However, until now the effects of finite relaxation times have not been considered. The CHESS sequence has extensively been investigated in terms of its dependence upon B_1 inhomogeneities and especially longitudinal T_1 relaxation (29, 30). Although SWAMP operates in a B_1 independent manner, the water suppression will undoubtedly be compromised by T_1 relaxation during the RF pulses and magnetic field gradients. Figure 6 shows simulations of SWAMP for $\gamma B_{1max} = \Delta\omega_{max}$ (=667 Hz) in the presence of finite T_1 and T_2 relaxation times. The finite longitudinal relaxation has two effects on the SWAMP suppression profile. First, the longitudinal magnetization for $|\Delta\Omega| < |\Delta\omega_{max}|$ rapidly relaxes during inversion (during and following the first and third AFP pulses). This leads to a decrease of the longitudinal magnetization at the end of SWAMP for $|\Delta\Omega| < |\Delta\omega_{max}|$. Second, the suppression profile becomes asymmetrical. For $\Delta\Omega = \Delta\omega_{max}$, the AFP pulse is essentially an AHP pulse and the longitudinal magnetization follows the effective field from the longitudinal axis to the transverse plane. For $\Delta\Omega = -\Delta\omega_{max}$, the magnetization will rotate about the effective field and will also assume negative z' values in the frequency frame $x'y'z'$ before ending up in the transverse plane. Therefore, longitudinal relaxation influences the profile more strongly for $\Delta\Omega = -\Delta\omega_{max}$ than for $\Delta\Omega = \Delta\omega_{max}$. Following identical arguments, it can also be explained that the profile around $\Delta\omega_{max}$ (or $-\Delta\omega_{max}$) becomes slightly asymmetrical (i.e., the point of optimal water suppression shifts to lower frequencies). For a practical implementation of SWAMP it is therefore recommended to use the suppression band at $+\Delta\omega_{max}$ for water suppression. In the presence of very short T_1 relaxation times it may be worthwhile to optimize the exact suppression frequency, although this did not improve the water suppression in the spectra presented in this study. For optimal water suppression, the duration of the magnetic field gradients should be minimized. When SWAMP is used in combination with STEAM localization (7), two or four AFP pulses may be placed in the TM period.

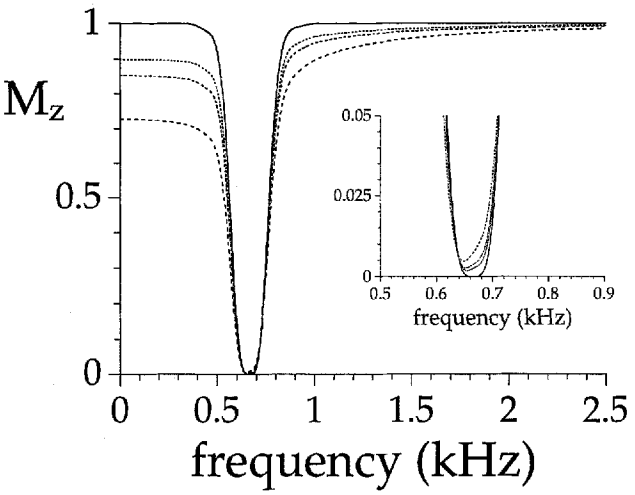

FIG. 6. Simulation of the longitudinal magnetization in the presence of longitudinal and transverse relaxation during SWAMP water suppression. SWAMP consisted of four hyperbolic-secant modulated AFP pulses (T = 15 ms, $\Delta\omega_{max}$ = 667 Hz, γB_{1max} = 667 Hz) interleaved by 1-ms magnetic field gradients. The simulations based on the Bloch equations were performed in the absence (solid line) and presence of relaxation (dashed lines). The ratio of longitudinal/transverse relaxation times was kept constant according to T_1/T_2 = 1500/150 ms (short dashed line), 1000/100 ms (medium dashed line) and 500/50 ms (long dashed line). The inset shows the longitudinal magnetization around the region of signal suppression at $\Delta\Omega = -\Delta\omega_{max}$.

The presence of short T_2 relaxation times has negligible effects on the longitudinal magnetization at the end of conventional RF pulses and is therefore often not considered in relation to water suppression. However, it is well known that short T_2 relaxation times degrade the inversion profile of AFP pulses (19, 21, 22, and references therein), i.e., the inversion for $|\Delta\Omega| < |\Delta\omega_{max}|$ is incomplete and the magnetization will not completely return to the longitudinal axis for $|\Delta\Omega| > |\Delta\omega_{max}|$. This is also observed for SWAMP as shown in Fig. 6, where short T_2 relaxation times lead to signal loss for $|\Delta\Omega| > |\Delta\omega_{max}|$ (i.e., in the frequency range of the metabolites in *in vivo* ^{1}H MR spectra). It is important to note that short T_2 relaxation times do not have any effect on the suppression efficiency of the water resonance. Since the signal loss for $|\Delta\Omega| > |\Delta\omega_{max}|$ increases with increasing RF amplitude, it is recommended to operate SWAMP in the low RF amplitude range. This is also recommended from the viewpoint of RF power deposition, which is an important consideration, especially in human studies. The hyperbolic-secant modulated AFP pulses used in SWAMP ($\Delta\omega_{max}T = 10$) need ≥10 times higher RF amplitude than Gaussian RF pulses of the same pulse length. Furthermore, the average RF power (calculated as the integral of $B_1(t)^2$) of an AFP pulse is ≥75 times higher than that of a Gaussian RF pulse. However, even though SWAMP has higher power requirements than CHESS, this does not have to limit the applications of SWAMP. Several research groups have used comparable AFP pulses for spatial localization on human brain and muscle (31–33), while keeping the RF power well within FDA guidelines for power absorption.

CONCLUSION

SWAMP achieves excellent B_1 insensitive water suppression without compromising the minimum attainable TR or TE. The removal of the 1% RF amplitude cut-off level of the AFP pulses results in a well-defined suppression frequency band and is highly recommended for all applications that use adiabatic pulses with an infinite RF amplitude modulation function. SWAMP is easy to implement and convenient with any type of RF coil since it only requires a one-time experimental optimization of the minimum RF amplitude.

REFERENCES

1. D. I. Hoult, Solvent peak saturation with single phase and quadrature Fourier transformation. *J. Magn. Reson.* **21,** 337–347 (1976).
2. R. K. Gupta, Dynamic range problem in Fourier transform NMR. Modified WEFT pulse sequence. *J. Magn. Reson.* **24,** 461–465 (1976)
3. P. Plateau, M. Gueron, Exchangable proton NMR without base-line distortion, using a new strong-pulse sequence. *J. Am. Chem. Soc.* **104,** 7310–7311 (1982).
4. P. J. Hore, Solvent suppression in Fourier transform nuclear magnetic resonance. *J. Magn. Reson.* **55,** 283–300 (1983)
5. A. Haase, J. Frahm, W. Hanicke, *D. Matthaei* ^{1}H NMR chemical shift selective (CHESS) imaging. *Phys. Med. Biol.* **30,** 341–344 (1985).
6. D. M. Doddrell, G. J. Galloway, W. M. Brooks, J. Field, J. U. Bulsing, M. G. Irving, H. Baddeley, Water signal elimination *in vivo*, using "suppression by mistimed echo and repetitive gradient episodes." *J. Magn. Reson.* **70,** 176–180 (1986)
7. C. T. W. Moonen, P. C. M. van Zijl, Highly effective water suppression for *in vivo* proton NMR spectroscopy (DRYSTEAM). *J. Magn. Reson.* **88,** 28–41 (1990).
8. P. C. M. van Zijl, C. T. W. Moonen, Complete water suppression for solutions of large molecules based on diffusional differences between solute and solvent (DRYCLEAN). *J. Magn. Reson.* **87,** 18–25 (1990).
9. M. Piotto, V. Saudek, V. Sklenar, Gradient-tailored excitation for single-quantum NMR spectroscopy of aqueous solutions. *J. Biomol. NMR* **2,** 661–665 (1992).
10. T.-L. Hwang, A. J. Shaka, Water suppression that works. Excitation sculpting using arbitrary waveforms and pulsed field gradients. *J. Magn. Reson A* **112,** 275–279 (1995).
11. M. Mescher, A. Tannus, M. O'Neil Johnson, M. Garwood, Solvent suppression using selective echo dephasing. *J. Magn. Reson. A* **123,** 226–229 (1996).
12. M. Gueron, P. Plateau, M. Decorps, Solvent signal suppression in NMR. *Prog. NMR Spectrosc.* **23,** 133–209 (1990)
13. J. E. Meier, A. G. Marshall, Methods for suppression of the H_2O signal in proton FT/NMR spectroscopy. A review, *in* "Biological Magnetic Resonance" (L. J. Berliner, J. Reuben, Eds.), vol. 9, pp. 199–240, Plenum Press, New York, 1990.
14. P. C. M. van Zijl, C. T. W. Moonen, Solvent suppression for *in vivo* magnetic resonance spectroscopy, *in* "NMR Basic Principles and Progress" (P. Diehl, E. Fluck, H. Gunther, R. Kosfeld, J. Seelig, Eds.), vol. 26, pp. 67–108, Springer-Verlag, Berlin, 1992.
15. W. Dreher, D. G. Norris, D. Leibfritz, Magnetization transfer affects the proton creatine/phosphocreatine signal intensity: *In vivo* demonstration in the rat brain. *Magn. Reson. Med.* **31,** 81–84 (1994)
16. R. A. de Graaf, A. van Kranenburg, K. Nicolay, Off resonance magnetization transfer measurements on rat brain *in situ*, in "Proc., ISMRM, 6th Annual Meeting, 1998," p. 329.
17. D. G. Schupp, H. Merkle, J. M. Ellerman, Y. Ke, M. Garwood, Localized detection of glioma glycolysis using edited ^{1}H MRS. *Magn. Reson. Med.* **30,** 18–27 (1993).
18. B. A. Inglis, K. D. Sales, S. C. R. Williams, BIRIANI: A new composite adiabatic pulse for water-suppressed proton NMR spectroscopy. *J. Magn. Reson.* **105,** 61–64 (1994).
19. R. A. de Graaf, Y. Luo, M. Terpstra, H. Merkle, M. Garwood, A new localization method using an adiabatic pulse, BIR- 4. *J. Magn. Reson. B* **106,** 245–252 (1995).
20. R. A. de Graaf, Y. Luo, M. Garwood, K. Nicolay, B_1-insensitive, single- shot localization and water suppression. *J. Magn. Reson. B* **113,** 35–45 (1996).
21. M. Garwood, K. Ugurbil, B_1 insensitive adiabatic RF pulses, *in* "NMR Basic Principles and Progress" (P. Diehl, E. Fluck, H. Gunther, R. Kosfeld, J. Seelig, Eds.), vol. 27, pp. 109–147, Springer-Verlag, Berlin, 1992.
22. R. A. de Graaf, K. Nicolay, Adiabatic rf pulses: Applications to *in vivo* NMR. *Concepts Magn. Reson.* **9,** 247–268 (1997).
23. M. S. Silver, R. I. Joseph, D. I. Hoult, Highly selective $\pi/2$ and π pulse generation. *J. Magn. Reson.* **59,** 347–351 (1984).
24. R. J. Ordidge, A. Connelly, J. A. B. Lohman, Image-selected *in vivo* spectroscopy (ISIS). A new technique for spatially selective NMR spectroscopy. *J. Magn. Reson.* **66,** 283–294 (1986).
25. R. Freeman, E. Kupce, Decoupling: Theory and practice. I. Current methods and recent concepts. *NMR Biomed.* **10,** 372–380 (1997).
26. A. Tannus, M. Garwood, Improved performance of frequency-swept pulses using offset-independent adiabaticity. *J. Magn. Reson. A* **120,** 133–137 (1996).
27. P. C. M. van Zijl, C. T. W. Moonen, *In situ* changes in purine nucleotide and N-acetyl concentrations upon inducing global ischemia in brain. *Magn. Reson. Med.* **29,** 381–385 (1993)
28. K. Ugurbil, M. Garwood, A. R. Rath, Optimization of modulation functions to improve insensitivity of adiabatic pulses to variations in B_1 magnitude. *J. Magn. Reson.* **80,** 448–469 (1988)
29. R. J. Ogg, P. B. Kingsley, J. S. W. E. T. Taylor, a T_1- and B_1-insensitive water-suppression method for *in vivo* localized ^{1}H NMR spectroscopy. *J. Magn. Reson. B* **104,** 1–10 (1994).
30. T. Ernst, J. Hennig, Improved water suppression for localized *in vivo* ^{1}H spectroscopy. *J. Magn. Reson. B* **106,** 181–186 (1995).
31. P. R. Luyten, J. P. Groen, J. W. A. H. Vermeulen, J. A. den Hollander, Experimental approaches to image localized human ^{31}P NMR spectroscopy. *Magn. Reson. Med.* **11,** 1–21 (1989).
32. R. Gruetter, E. J. Novotny, S. D. Boulware, G. F. Mason, D. L. Rothman, G. I. Shulman, J. W. Prichard, R. G. Shulman, Localized ^{13}C NMR spectroscopy in the human brain of amino acid labeling from D-[1–13C]glucose. *J. Neurochem.* **63,** 1377–1385 (1994).
33. R. Gruetter, G. Adriany, H. Merkle, P. M. Andersen, Broadband decoupled ^{1}H-localized ^{13}C MRS of the human brain at 4 Tesla. *Magn. Reson. Med.* **36,** 659–664 (1996).